Check for updates

AGU ADVANCING EARTH AND SPACE SCIENCE

Water Resources Research

RESEARCH ARTICLE
10.1029/2021WR029625

An Eulerian Model for the Transport and Diffusion of Floating Particles Within Regions of Emergent Vegetation

Wei Shi[1], Paolo Peruzzo[1], and Andrea Defina[1]

[1]Department of Civil, Environmental and Architectural Engineering, University of Padova, Padova, Italy

Wei Shi and Paolo Peruzzo contributed equally to this paper.

Key Points:

- The use of a Lagrangian model to simulate particles propagation is demanding on computation and an Eulerian approach is far preferable
- The proposed Eulerian scheme is more effective to describe the transport and diffusion of particles, such as seeds, in vegetated areas
- In presence of diffusion and permanent capture of particles by plants, the parameters of the Eulerian model become time-dependent

Correspondence to:
P. Peruzzo,
paolo.peruzzo@dicea.unipd.it

Citation:
Shi, W., Peruzzo, P., & Defina, A. (2021). An Eulerian model for the transport and diffusion of floating particles within regions of emergent vegetation. *Water Resources Research*, *57*, e2021WR029625. https://doi.org/10.1029/2021WR029625

Received 15 JAN 2021
Accepted 16 JUL 2021

© 2021. The Authors.
This is an open access article under the terms of the Creative Commons Attribution License, which permits use, distribution and reproduction in any medium, provided the original work is properly cited.

Abstract Emergent vegetation has a significant impact on floating particle transport and diffusion in open channel flow. The random walk model of a Lagrangian approach has proven more than suitable to describe the rather unpredictable moving trajectory of particles within emergent vegetation. However, compared to the large computational costs of the Lagrangian model, which also requires more input data, a simplified model based on the Eulerian approach can be by far preferable and cost-effective for rapid first-order prediction of particle transport and diffusion within vegetated areas. In this study, we developed a one-dimensional advection-diffusion model to simulate particle transport processes within vegetated areas, and to explore the impacts of vegetation on particles transport, diffusion and removal. The model parameters, including the probability of a particle colliding with a stem, and the probability of it being temporarily trapped or permanently captured by a stem, as well as the mean retention time that govern the random walk model, are introduced to estimate the mean velocity, diffusion coefficient, removal rate of particles of Eulerian model, distinguishing from the standard advection and diffusion parameters. The validity of the parameters is verified through the stochastic model with a large number of realizations. The comparison between the dispersal kernel as well as the spatio-temporal distribution of floating particles predicted by Eulerian model and stochastic model is quite satisfactory and suggests that the Eulerian model we proposed is properly described.

1. Introduction

The transport, retention, and deposition of organic matter, whether it be seeds, propagules, or small eggs, are fundamental processes for wetlands ecosystems (Merritt & Wohl, 2002; Nilsson et al., 2010; Peterson & Bell, 2012). The transport of particles within vegetated areas is a rather complex problem. On one hand, plants increase vertical diffusivity and thus reduce the longitudinal hydrodynamic dispersion (Nepf, Mugnier, & Zavistoski, 1997; Nepf, 1999). On the other hand, the interactions with the vegetation strongly affect the fate of particles, promoting their retention, as well as the mechanical dispersion, due to the different paths traveled by particles through the canopy (Chang et al., 2008; Nepf, Mugnier, & Zavistoski, 1997).

Depending on the particle and plant characteristics, the mechanisms of interaction can be manifold. For instance, plants can directly intercept small heavier-than-water or neutrally buoyant particles, such as sediments or seeds, or exploit other mechanisms such as electrostatic attraction or retention due to the recirculating zone in the wake behind the stems (Espinosa-Gayosso et al., 2013; Rubenstein & Koehl, 1977; Shimeta & Jumars, 1991; White & Nepf, 2003). Floating particles are also subjected to the capillary force arising from the interaction between the menisci of both the floating body and piercing-surface stems (Chambert & James, 2009; Peruzzo et al., 2013; Vella & Mahadevan, 2005). In addition, the large-size particles are slowed down when colliding with the plant because of their inertia, or they are arrested by the plants' net-like structure, that is, the so-called net trapping mechanism (Defina & Peruzzo, 2010).

The trajectory of a particle flowing and slaloming through emergent vegetation is thus rather unpredictable, and a stochastic approach to describe particle propagation is preferable. Defina and Peruzzo (2010) proposed a specific random walk model in order to study the transport of floating particles within a canopy of mimicked vegetation. In the model, the path traveled by a particle through emergent vegetation is described according to a Lagrangian approach. The mechanisms leading a particle to collide with or be retained by the vegetation are not described in detail, but the effects of vegetation on the propagation of a particle are taken into account by introducing a set of probabilities to assess how often the particle may interact with,

and then either be permanently captured or temporarily trapped by the stems. Although purely stochastic in the model, the probabilities of interaction and retention of the particle are actually closely related to the collision efficiency of the stem (η, defined as the ratio of span within which particles can collide with the stem and the stem diameter, where this span is dependent on hydrodynamics) (Espinosa-Gayosso et al., 2015; Liu et al., 2018; Palmer et al., 2004; Peruzzo et al., 2012, 2016). Specific experiments have also been carried out to assess the retention time of floating particles in different flow conditions, highlighting the existence of two retention time-scales. Short retention times are associated with the slow-down process that a particle experiences when it hits a stem, rolls around it and interacts with its wake before it continues to move downstream; long retention times are associated with the temporary trapping of particles by capillarity or through the net trapping mechanism (Peruzzo et al., 2012).

To date, the Lagrangian stochastic approach has proven more than suitable to describe the propagation of particles and their interactions with the vegetation. However, the Lagrangian stochastic model is extremely demanding, both on input data and computational costs at large scales. To overcome this drawback, whenever possible, upscaling from the local interaction processes between particles and stems is desirable, and this means moving from the Lagrangian to the Eulerian approach.

Advection-diffusion models have been widely and successfully applied to describe the transport of particles through vegetation by assuming that the particle transport is driven by the mean flow velocity (Cunnings et al., 2016; Nepf, Mugnier, & Zavistoski, 1997; Nitto et al., 2013; Richards et al., 1995; Shi et al., 2020). Recently, Liu et al. (2020) assessed an Eulerian model including the mechanical dispersion due to the slow-down of particles interacting with the vegetation stems, but to the best of our knowledge, an advection-diffusion model that includes long-time retention mechanisms is lacking. Note that long-time retention is often the main process promoting particle dispersion at large scales.

This study aims at covering this gap in knowledge by presenting an advection-diffusion model, whose parameters are strictly related to those of the Lagrangian stochastic model proposed by Defina and Peruzzo (2010), which also accounts for long-time retention processes and particle removal by vegetation.

2. Methods

Since we want to develop an Eulerian model whose parameters are strictly related to those of the Lagrangian stochastic model, a short description of the latter model is given below. It is also worth pointing out that the stochastic model, originally developed to describe the transport and diffusion of floating particles, can be applied also to the case of moderately heavier than water or neutrally buoyant particles.

2.1. The Stochastic Model

The stochastic model, proposed by Defina and Peruzzo (2010), considers the generic trajectory traveled by a particle with velocity U within a region of emergent vegetation; the trajectory is dissected into segments or sections with length $\Delta s = 1/\sqrt{n}$, n being the stem density. Within each section, the particle has the probability P_i of interacting with a stem, and probability $1 - P_i$ of flowing downstream undisturbed.

When a particle collides with a stem, it can be slowed down, with probability P_s; temporarily trapped, with probability P_t; or permanently captured, with probability P_c. When a particle is temporarily trapped, it stays on place for a random time. Based on the experimental results of Defina and Peruzzo (2012), we can assume, as a good approximation, this random time is exponentially distributed with a mean value, T. Details on the mechanisms that cause temporary or permanent captures can be found in Defina and Peruzzo (2010, 2012). The layout of the model is shown in Figure 1.

The typical time delay in the particle propagation produced by slow-down events is of order one second, which is much shorter than temporary trapping events (Defina & Peruzzo, 2010; Liu et al., 2020). Accordingly, and for the sake of simplicity, slow-down events are neglected in this work, that is, when a slow-down event is predicted to occur, with probability $P_s = 1 - P_t - P_c$, we assume that the particle behaves as if it did not interact with the stem at all.

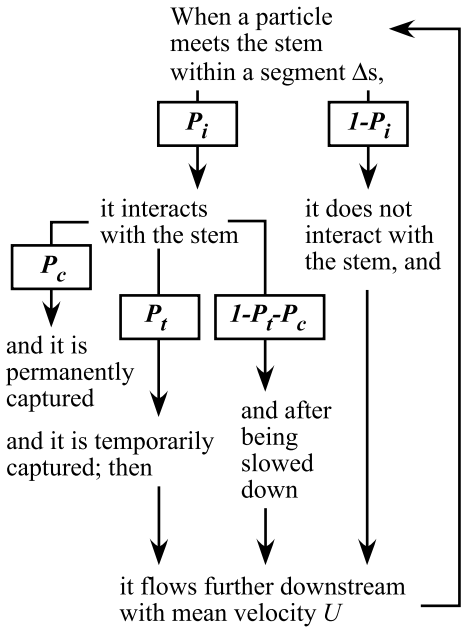

Figure 1. Layout of the stochastic model, adapted from Defina and Peruzzo (2010).

2.2. The Eulerian Model

Modeling the large-scale dispersal of particles within regions of emergent vegetation with the Lagrangian stochastic model is extremely burdensome, and a model based on the Eulerian approach is far preferable. The problem then consists of relating the parameters of the stochastic model, namely, P_i, P_c, P_t, T, U, and n or Δs, to the parameters of a standard transport and diffusion model, including a first-order decay

$$\frac{\partial c}{\partial t} + U_m \frac{\partial c}{\partial x} - D\frac{\partial^2 c}{\partial x^2} = -\varphi c, \tag{1}$$

where c and U_m are the particle concentration and the mean transport velocity, respectively, D is the longitudinal diffusion coefficient; and φ is the capture rate coefficient that controls the fraction of particles that are permanently captured by vegetation per unit time.

The propagation of the particles described by Equation 1 is 1D with the x-direction corresponding to the local streamwise direction, which is also the direction of the principal axis of inertia. Accordingly, the 1D model can easily be extended to the 2D case once specified the diffusion in the transverse direction (e.g., as found by Nepf, Sullivan, and Zavistoski (1997)) that allows to construct the 2D diffusion tensor.

The spatial distribution of permanently captured particles can then be estimated as

$$\frac{\partial c_p}{\partial t} = \varphi c, \tag{2}$$

with c_p the concentration of permanently captured particles.

As stated above, the three parameters introduced in Equation 1, namely, U_m, D and φ, need to be assessed by relating them to the parameters governing the stochastic model. For this purpose, the results of the stochastic model are compared with the analytical solution of Equation 1. In particular, the propagation of a cloud of particles, of unit mass, released in $x = 0$ at $t = 0$ is simulated with the stochastic model. The solution to Equation 1, by prescribing $c(\pm\infty,t) = 0$ as boundary condition, and $c(x,0) = \delta(x)$, with $\delta(x)$ the Dirac delta function, as initial condition, reads

$$c(x,t) = \frac{1}{\sqrt{4\pi D t}} \exp\left[-\frac{(x - U_m t)^2}{4Dt} - \varphi t\right]. \tag{3}$$

It is worth noting that, since the mass is unitary, at each instant t the concentration $c(x,t)$ represents the probability density function of the particle position.

The transport velocity $\boldsymbol{U_m}$. Along a generic trajectory of length L through the stem array, a particle is assumed to step through $m_0 = L / \Delta s$ sections, each containing one stem; at each step, the probability that a particle collides with the stem and remains temporarily trapped is $P_i P_t$. Let T be the mean retention time, that is, the mean time a particle remains attached to a stem at each temporary trapping event. Then the mean time, Δt, taken by a particle to traverse the length Δs is given by the sum of the travel time, $\Delta s / U$, and the retention time, $P_i P_t T$ weighted by the fraction $(1 - P_i P_c)$ of active particles, that is, particles that are not removed from the flow by being permanently captured by vegetation

$$\Delta t = \frac{\Delta s}{U} + \frac{P_i P_t T}{1 - P_i P_c},$$

where U is the particle velocity while freely flowing downstream without any interaction; this velocity can be approximated with the bulk flow velocity. The above equation can be rearranged to read

$$\Delta t = \frac{\Delta s}{U}(1 + \omega), \tag{4}$$

with

$$\omega = \frac{P_i P_t}{1 - P_i P_c} \frac{UT}{\Delta s}.$$

The mean transport velocity U_m, that is, the mean velocity of a particle including its temporary stops, is then given by

$$U_m = \frac{\Delta s}{\Delta t} = \frac{1}{1+\omega} U. \tag{5}$$

The parameter $\boldsymbol{\varphi}$. To assess the parameter φ, we refer to the case without diffusion in the Eulerian model, and hence without temporary trapping events in the stochastic model, and consider the spatial distribution of permanently captured particles as time goes to infinite; in this case, $c_p(x, t \to \infty)$ follows an exponential law (Peruzzo et al., 2012)

$$c_p(x, t \to \infty) = \frac{1}{\lambda} e^{-L/\lambda}, \tag{6}$$

where

$$\lambda = -\frac{\Delta s}{\ln(1 - P_i P_c)}.$$

When $t < \infty$, the distribution is given by the previous equation truncated at the distance $x = Ut$, that is,

$$c_p(x,t) = \begin{cases} \frac{1}{\lambda} e^{-L/\lambda} & x \le Ut \\ 0 & x > Ut \end{cases}. \tag{7}$$

In the absence of diffusion ($D = 0$) and of temporary trapping events ($P_t = 0$) the transport velocity U_m reduces to U, as stated by Equation 5 and 1 is rewritten as

$$\frac{\partial c}{\partial t} + U \frac{\partial c}{\partial x} = -\varphi c. \tag{8}$$

With the initial condition given by the Dirac delta function, $c(x, 0) = \delta(x)$, and boundary condition $c(\pm\infty, t) = 0$, the solution of the above equation reads

$$c(x,t) = e^{-\varphi t} \delta(x - Ut). \tag{9}$$

With this distribution of particles concentration, and assuming $c_p(x, 0) = 0$, Equation 2 can be solved to give

$$c_p(x,t) = \frac{\varphi}{U} e^{-\varphi x/U} H(t - x / U), \tag{10}$$

where $H(x)$ is the Heaviside step function. Equivalently, Equation 10 can be written as

$$c_p(x,t) = \begin{cases} \frac{\varphi}{U} e^{-\varphi x/U} & x \le Ut \\ 0 & x > Ut \end{cases}. \tag{11}$$

From the comparison of the above Eulerian solution with the solution of the stochastic model given by Equation 7, we have

$$\varphi = \frac{U}{\lambda} = -\frac{U}{\Delta s} \ln(1 - P_i P_c). \tag{12}$$

We recall that the velocity U in the above equation is actually the transport velocity U_m that reduces to U when the diffusion is negligible. Consequently, in the presence of diffusion and temporary trapping events, the capture rate coefficient is still given by Equation 12 provided that the velocity U is replaced with U_m.

The diffusion coefficient $\boldsymbol{D}$. The diffusion of particles transported in a turbulent flow is mainly due to the mixing mechanism promoted by turbulence. However, in vegetated flows there are additional mechanisms acting to enhance dispersion (Nepf, Mugnier, & Zavistoski, 1997; White & Nepf, 2003). One mechanism is associated with the back-flow region within the wake behind the plant stems that may temporarily detain

the flowing particles; this mechanism turns out to be effective only when the particle size is much smaller than the stem diameter. A more effective mechanism, which produces the so-called mechanical or hydrodynamic dispersion, arises because of the non-uniform transport velocity within the stem array, and the different length of the paths traveled by the particles while slaloming through the stems (Nepf, Mugnier, & Zavistoski, 1997). In the case of floating particles, the temporary trapping by capillarity or by net trapping mechanism, and the associated time delay taken by particles to propagate, largely enhances the longitudinal dispersion.

The probability that a floating particle experiences k temporary trapping events while traversing m_0 sections of length Δs, has a binomial distribution (Nepf, Mugnier, & Zavistoski, 1997)

$$P(k) = C_{m_0}^{k}\left(\frac{P_i P_t}{1 - P_i P_c}\right)^{k}\left(1 - \frac{P_i P_t}{1 - P_i P_c}\right)^{m_0 - k}, \tag{13}$$

with $C_{m_0}^{k}$ the binomial coefficient. The mean number of delays is $m = m_0 P_i P_t \,/\, (1 - P_i P_c)$, and the variance is

$$\sigma_{m_0}^{2} = m_0 \frac{P_i P_t}{1 - P_i P_c}\left(1 - \frac{P_i P_t}{1 - P_i P_c}\right). \tag{14}$$

After experiencing a moderately large number of sections, the binomial distribution tends toward a normal distribution with the same mean and variance; accordingly, for the case of a cloud of particles released just upstream of the vegetated area, with zero variance, after a period of time $t = m_0 \Delta t$, the spatial variance will be

$$\sigma^2(t) = \ell^2 \sigma_{m_0}^{2}, \tag{15}$$

with ℓ a suitable longitudinal length. In addition, the variance grows linearly with time as (Fischer et al., 1979; Rutherford, 1994):

$$\sigma^2(t) = 2Dt, \tag{16}$$

with D the diffusion coefficient. We further assume $\ell = \ell_0 U_m T$, with ℓ_0 a calibration factor, and combine Equations 5 and 14–16 to yield

$$D = \ell_0^2 \frac{1 - \dfrac{P_i P_t}{1 - P_i P_c}}{2} \frac{\omega}{(1+\omega)^3} U^2 T. \tag{17}$$

By comparing the concentration distribution provided by the stochastic model with that provided by the Eulerian model, we find $\ell_0^2 = (2 - \dfrac{P_i P_t}{1 - P_i P_c}) \,/\, (1 - \dfrac{P_i P_t}{1 - P_i P_c})$, and hence, we obtain

$$D = \left[1 - \frac{P_i P_t}{2(1 - P_i P_c)}\right] \frac{\omega}{(1+\omega)^3} U^2 T. \tag{18}$$

The above diffusion coefficient can be added to those stemming from other mechanisms promoting particle dispersal, for example, mechanical and turbulent diffusion (Nepf, Mugnier, & Zavistoski, 1997). As it will be shown in Section 3, the long time trapping mechanism is prevalent in most cases, so that the other mechanisms promoting diffusion can be often neglected.

Overall, the parameters of the Eulerian model are given by the following set of relationships

$$\begin{cases} U_m = \dfrac{U}{1+\omega} \\ D = \left[1 - \dfrac{P_i P_t}{2(1 - P_i P_c)}\right] \dfrac{\omega}{(1+\omega)^3} U^2 T \\ \varphi = -\dfrac{U_m}{\Delta s} \ln(1 - P_i P_c) \end{cases}. \tag{19}$$

The reliability of the solution here proposed, that is, Equation 19, will be assessed in the next Section through the comparison of the predictions of the two approaches; in this regard, a simple non-dimensional analysis of the parameters of the stochastic model is useful. The stochastic model is governed by the parameters P_i,

P_t, P_c, U, Δs, and T; these parameters can be grouped as P_iP_t, P_iP_c, and UT / Δs. In this way, the parameters of the Eulerian model, in non-dimensional form, that is, U_m / U, D / U^2T, and φT, as given by Equation 19, can all be written as a function of the above three non-dimensional parameters.

3. Results and Discussion

In this Section, the results of the application of the stochastic model are compared with the solution of the Eulerian model. In particular, the propagation of a cloud of particles released in $x = 0$ at $t = 0$ is simulated both by the stochastic and the Eulerian model.

The diffusion process described by the Lagrangian stochastic model can be considered as Fickian once all the particles experience a sufficient number of interactions. In fact, at the very beginning of the propagation process, a fraction of the cloud of particles has never interacted with the vegetation and hence has moved downstream with velocity U; all these particles, at the generic instant, t, are accumulated at $x = Ut$ and the spatial distribution of the concentration is there truncated. We then need that this fraction of particles be extremely small and hence negligible. The fraction of particles, C, that at time t has not yet interacted with any stem is

$$C = (1 - P_iP_c - P_iP_t)^{\frac{UT}{\Delta s}\frac{t}{T}}. \tag{20}$$

Let C_{min} be the fraction of particles that can be assumed negligibly small; according to Equation 20 we have

$$\frac{t}{T} > \frac{ln(C_{min})}{\frac{UT}{\Delta s} ln(1 - P_iP_c - P_iP_t)}. \tag{21}$$

From the analysis of the results provided by the stochastic model, $C_{min} = 10^{-4}$ is found to be an acceptable threshold. An additional and independent lower boundary for the relative time t / T stems from the requirement that the initial binomial distribution must have time to evolve and approach a Gaussian distribution; this occurs when t / $T > 10 - 20$.

If $P_c > 0$, the progressive reduction of the number of the uncaptured particles makes the statistical analysis of the results, provided by the Lagrangian stochastic model, extremely demanding, particularly in the last stage of depletion of the transport process. For this reason, it is useful to consider an upper limit for the relative time t / T. A simple estimate of the number of uncaptured particles as time progresses is given by the spatial integration of Equation 11 that yields

$$C_p = 1 - e^{-\varphi t}. \tag{22}$$

Actually, Equation 11, and hence Equation 22, can be established when diffusion is neglected; however, the results of the present numerical analysis show that Equation 22 provides a sufficiently accurate estimate even in the presence of diffusion. In this study, the statistical analysis is limited by relative times such that $C_p \leq C_{p\,max}$, with $C_{p\,max} \approx 95\%$. Combining Equation 19 for φ with Equation 22, this condition can be rewritten as

$$\frac{t}{T} \leq \frac{1 - P_iP_c + P_iP_t}{(1 - P_iP_c) ln(1 - P_iP_c)} ln(1 - C_{p\,max}). \tag{23}$$

It is worth stressing that constraint Equation 23 does not necessarily need to be satisfied. Nevertheless, it must be said that, when the fraction of uncaptured particles is very small, for example, smaller than 5%, the relative error might be non-negligible while the absolute error is; this is the reason we confidently limited the statistical analysis to relative times that satisfy the above constraint.

In the stochastic model, the non dimensional parameters P_iP_t, P_iP_c, and UT / Δs are allowed to vary in the following ranges

$$0 \leq P_iP_t \leq 0.9, \qquad 0 \leq P_iP_c \leq 0.1, \qquad 0 \leq UT / \Delta s \leq 10^3. \tag{24}$$

The transport velocity $\boldsymbol{U_m}$. Figure 2 compares the mean transport velocity U_m given by the Equation 5 with the mean transport velocity U_{ms} computed with the stochastic model. After a relatively short initial time,

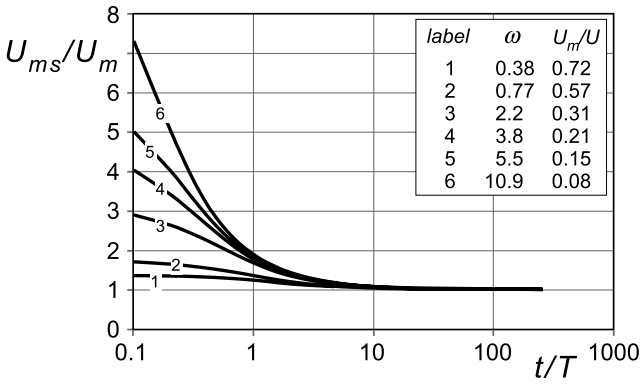

Figure 2. The ratio U_{ms} / U_m between the transport velocity computed with the stochastic model and that given by Equation 5 as a function of the relative time t / T. U_{ms} has been determined by averaging over 10^5 realizations.

t / $T \cong 10$, the transport velocity predicted by Equation 5 well corresponds to the one computed with the stochastic model. On the contrary, at the very early stage of the simulations, advection is the only process affecting the fate of the particles in the Lagrangian scheme, since only a small fraction of the particles interact with the vegetation. In this condition, that is, when t / $T \ll 1$, the velocity of the cloud centroid is close to U and hence $U_{ms}U_m \cong 1 + \omega$.

The capture coefficient $\boldsymbol{\varphi}$. To check the validity of Equation 12, predicting the parameter φ, we compare, in the absence of diffusion and temporary trapping processes, the spatial distribution of the permanently captured particles, c_p, computed with the stochastic model to that given by the Eulerian model, which is also referred to as dispersal kernel (Nathan & Muller-Landau, 2000). Figure 3 shows an example, among the many comparisons performed, of the fate of one cloud of 500 particles; the good agreement generally found between the analytical solution of the Eulerian model, given by Equation 11, and the results provided by the stochastic model, confirms the correctness of Equation 12.

In the presence of temporary trapping events, and hence of diffusion, we cannot compare the distribution $c_p(x,t)$ computed with the stochastic model with the solution of Equation 2 since no analytical solution of this equation is available when the distribution $c(x,t)$ is that given by Equation 3; in this case, the validity of Equation 12 is checked by estimating with the two models the amount of captured particles at different times. This procedure is illustrated later in the text.

The diffusion coefficient $\boldsymbol{D}$. The validity of Equation 18 relating the diffusion coefficient to the parameters of the stochastic model is preliminarily checked when the permanent capture is inhibited, that is, $\varphi = 0$ in Equation 1 and $P_c = 0$ in the stochastic model. In this case, if we release a cloud of particles with zero variance just upstream of the stem array ($x = 0$), at $t = 0$, the variance, σ^2, of the cloud grows linearly in time according to Equation 16.

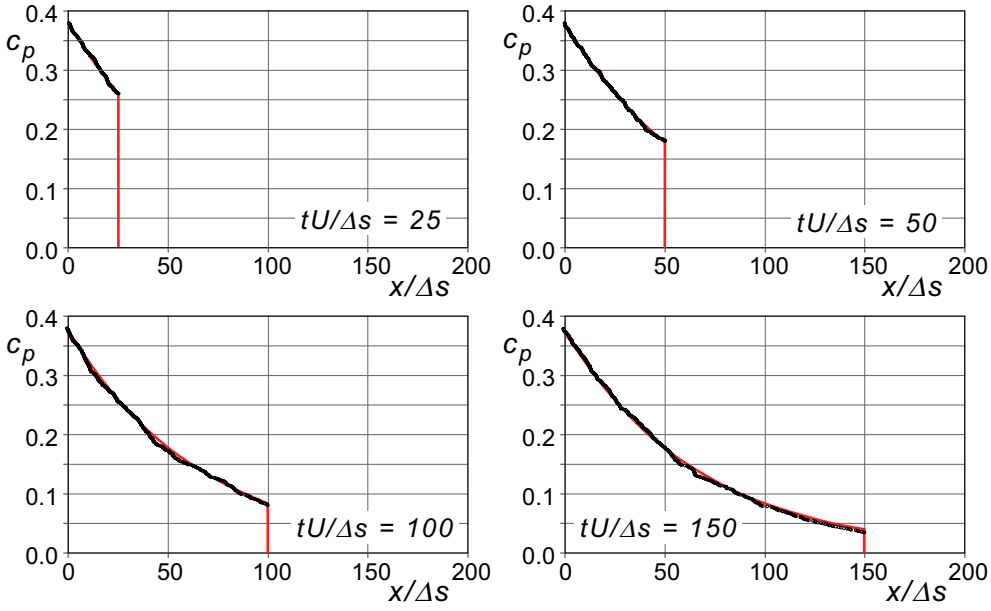

Figure 3. Example of the spatial distribution of captured particles concentration, c_p, at different times tU / Δs; the analytical solution of the Eulerian model, given by Equation 11 and denoted with red lines, is compared to the results provided by the stochastic model, denoted with small black dots. In this example the parameters of the stochastic model are $U = 0.05$ m/s, $n = 625$ m^{-2} and hence $\Delta s = 0.04$ m, $P_i = 0.3$, $P_c = 0.05$, and $P_t = 0$. The concentration $c_p(x,t)$ computed with the Lagrangian model is estimated by releasing one cloud of 500 particles.

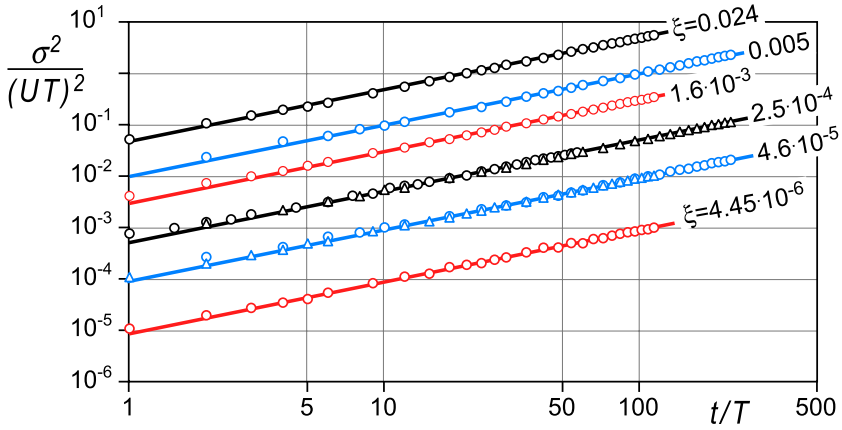

Figure 4. Comparison between diffusion predicted by the stochastic model and that computed with the Eulerian approach by demonstrating the non-dimensional variance $\sigma^2(UT)^2$ varies with time $t\ /\ T$ for some values of the coefficient ξ. In the Lagrangian model, the variance has been determined by averaging over 10^4 realizations.

Let ξ be the relative diffusion coefficient, $\xi = D\ /\ (U^2T)$; according to Equation 18 we have

$$\xi = \left[1 - \frac{P_i P_t}{2(1 - P_i P_c)}\right] \frac{\omega}{(1+\omega)^3}, \tag{25}$$

and Equation 16 can be rewritten as

$$\frac{\sigma}{UT} = \sqrt{2\xi}\sqrt{\frac{t}{T}}. \tag{26}$$

Figure 4 shows some examples of the non-dimensional variance $\sigma^2(UT)^2$ as it varies with the relative time $t\ /\ T$ for some values of the coefficient ξ; the results of the stochastic model, denoted with different symbols, strictly overlap the continuous curves given by Equation 26, with minor differences when $t\ /\ T < 5$.

The ability of Equation 18 to predict the diffusion coefficient is also checked by comparing the results provided by the stochastic model with the solution given by Equation 3 under different conditions.

The concentration distribution. An example of the comparison between the particle concentration distributions computed with the Lagrangian and the Eulerian models at different relative times, $t\ /\ T$, when the capture process is inhibited ($P_c = 0$) is shown in Figure 5. The Gaussian solution satisfactorily predicts the particle distribution, despite the slight positive asymmetry that does not allow the model to perfectly capture the tails of the concentration. The fit between the computed and predicted concentration improves with increasing $t\ /\ T$, as the equilibrium condition between longitudinal advection and retention is approached. It is worth noting, in Figure 5b, that when $t\ /\ T = 5$ the distribution $c(x,t)$ is truncated at $x = 5UT$; this is consistent with Equation 20 that gives $C = 8.6{\cdot}10^{-3} \gg C_{min} = 10^{-4}$. With the data of this example, the concentration is approximately distributed as a Gaussian when $t\ /\ T > 9.7$ as given by Equation 21.

As an example, Figure 6 compares the particle concentration distributions computed with the Lagrangian and the Eulerian models at different relative times, $t\ /\ T$, when the permanent capture process is allowed. Although the probability P_c is relatively small ($P_c = 2\%$ in panel *a*) and $P_c = 5\%$ in panel *b*)), the number of flowing particles reduces quite rapidly. Importantly, we observe that the cloud centroid is slightly slower than that computed when $P_c = 0$; however, also in this more complex scenario, the Eulerian solution describes satisfactorily the time evolution of the particle concentration. In this example, as well, when $P_c = 5\%$ (Figure 6b), the spatial distribution of the uncaptured particles at $t\ /\ T = 5$ is truncated at $x = 5UT$ for the same reason discussed above.

The many simulations and comparisons performed allow us to conclude that when $t\ /\ T > 10$ and $P_c = 0$ the transport velocity and the diffusion coefficient provided by the stochastic model are ultimately time-independent. For this reason, the values of these parameters computed with the stochastic model when $t\ /\ T > 10$ can confidently be compared with the corresponding theoretical values.

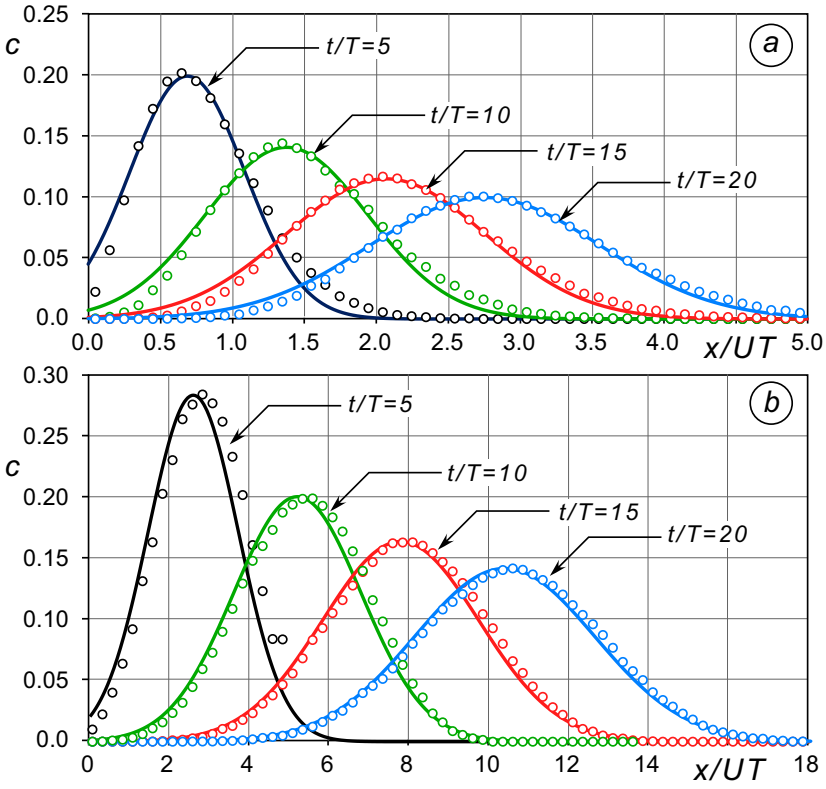

Figure 5. The spatial distribution of particle concentration at different times t / T; the analytical solution of the Eulerian model, denoted with thick lines, is compared to the results provided by the stochastic model, denoted with circles. In these examples the permanent capture is inhibited by assuming $P_c = 0$; the other parameters of the stochastic model are $U = 0.05$ m/s, $n = 625$ m^{-2} and hence $\Delta s = 0.04$ m, $P_i = 0.1$, *a*) $P_t = 0.5$, $T = 100$ s, and *b*) $P_t = 0.3$, and $T = 25$ s. The concentration $c(x,t)$ computed with the Lagrangian model is averaged over 10^5 runs.

Figure 7 compares the relative transport velocity U_m / U and the non dimensional diffusion coefficient D / U^2T computed with Equations 5 and 18, respectively, with the corresponding parameters, denoted with U_{ms} / U and D_s / U^2T, evaluated with the stochastic model at $t / T = 20$ when the permanent capture is inhibited: the agreement is very good.

It is worth noting that, regardless the presence of the permanent capture process, the interaction between particles and vegetation, and in particular, slow-down and temporary capture processes, promotes the reduction of the particles average velocity, that is, the transport velocity, that can be one order of magnitude smaller than the mean flow velocity. This important effect of the particle-vegetation interaction is often neglected in the standard advection-diffusive models, in which $U_m \approx U$ is assumed.

In the contemporary presence of temporary and permanent capture events things become complicated. A first important consequence is that the parameters of the Eulerian model become time dependent. Figure 8 shows an example of how the transport velocity U_m varies with time, from $t / T \approx 10$ to the upper boundary, given by Equation 23, and corresponding to when 95% of particles are permanently captured. Accordingly, the transport and diffusion process described by the Lagrangian stochastic model could not be transposed into an equivalent standard Eulerian model.

To make this point more clear, let us consider the case when permanent capture is inhibited. After some initial time, an equilibrium condition is reached so that the rate at which particles become temporarily trapped equals the rate at which temporarily trapped particles become free again and flow downstream with velocity U. On the contrary, when both temporary and permanent capture events affect the particle flow, the above equilibrium condition cannot be achieved. This is because the number of uncaptured particles reduces in time so that the number of particles that become temporarily trapped at time t is smaller than the number

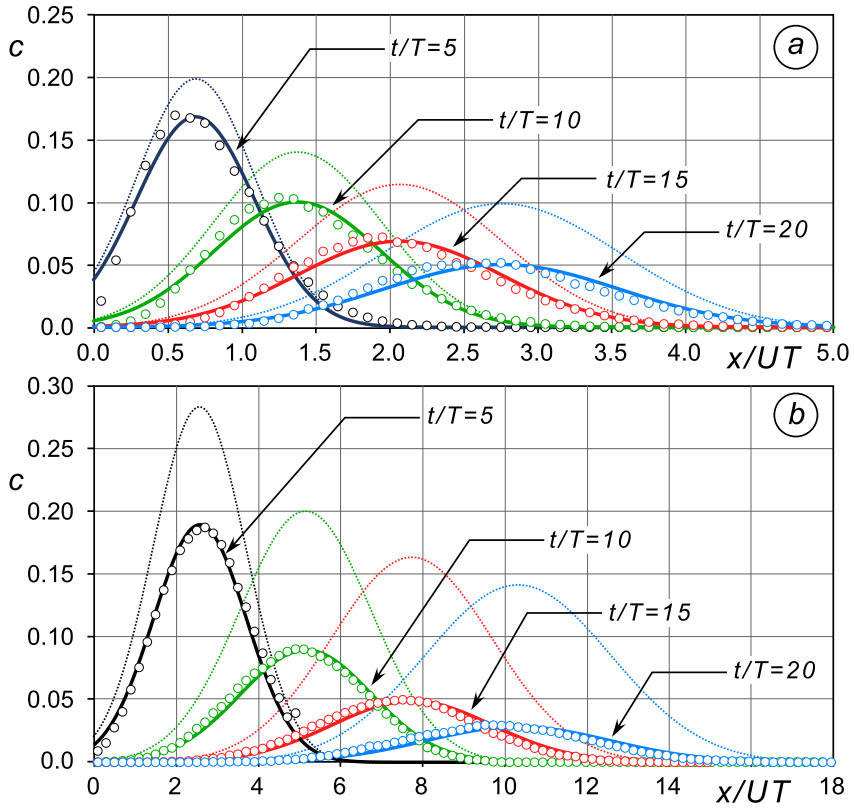

Figure 6. The spatial distribution of particle concentration at different times t / T; the analytical solution of the Eulerian model, denoted with thick lines, is compared to the results provided by the stochastic model, denoted with circles. In both these examples $U = 0.05$ m/s, $n = 625$ m^{-2} and hence $\Delta s = 0.04$ m, $P_i = 0.1$, whereas $P_t = 0.5$, $P_c = 0.02$, and $T = 100$ s are assumed for the case *a*); $P_t = 0.3$, $P_c = 0.05$, and $T = 25$ s, are assumed for the case *b*). Thin dotted lines are used to show the spatial distribution of particle concentration when P_c is set to zero. The concentration $c(x,t)$ computed with the Lagrangian model is averaged over 10^5 runs.

of particles, previously trapped, that become free again at time t. This mechanism promotes the reduction of the number of particles that are temporarily trapped at time t. However, the number of uncaptured particles reduces faster so that, as time progresses, the ratio of particles that are staying temporarily trapped to those

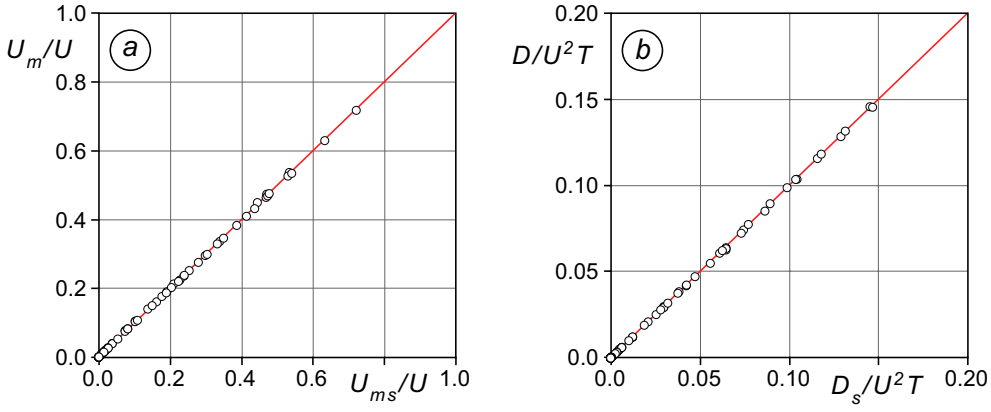

Figure 7. Comparison between the relative transport velocity U_m / U (panel a) and the non dimensional diffusion coefficient D / U^2T (panel b) computed with Equations 5 and 18, respectively, with the corresponding parameters, denoted with U_{ms} / U and D_s / U^2T, evaluated with the stochastic model at $t / T = 20$ when $P_c = 0$. In both plots, the coefficient of determination, R^2, is larger than 0.99.

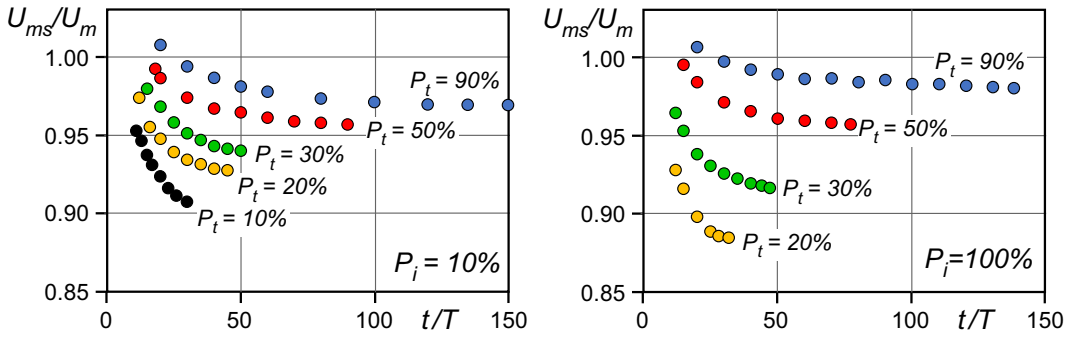

Figure 8. The ratio between the transport velocity computed with the stochastic model, U_{ms}, and the one given by Equation 5, as a funtion of the relative time, $t\ /\ T$; in both panels $P_c = 2\%$ and $UT\ /\ \Delta s = 100$. Relative time varies from $t\ /\ T \approx 10$ to the upper boundary, given by Equation 23.

that are freely flowing increases and hence the mean velocity, that is, the transport velocity, U_m, reduces in time. The same mechanism is responsible for the time reduction of the diffusion coefficient.

This point is rather interesting since we can state that the transport and diffusion process that includes some decay has memory of its previous conditions. Therefore, when modeling scenarios where the rate of permanent capture is relevant, an Eulerian model should strictly account for the history of particles propagation. However, the differences between the Lagrangian and the proposed Eulerian solutions are moderately small, especially when compared with the uncertainties that typically affect the estimation of the transport velocity and diffusion coefficient when dealing with the flow through vegetated areas.

Figure 9 collects the results of more than 400 cases with P_iP_c, P_iP_t, and $UT\ /\ \Delta s$ varying in the ranges given by Equation 24, and for different values of the relative time $t\ /\ T$. Black circles denote all cases when the relative time is in the range bounded by the lower and upper limits given by Equations 21 and 23, respectively; gray circles denote cases when the upper constraint for $t\ /\ T$, that is, Equation 23, is violated, whereas small white circles denote cases when the lower constraint Equation 21 is violated.

Figure 9a shows the ratio between the transport velocity computed with the stochastic model, U_{ms}, and the one given by Equation 5, as a function of $P_iP_c\ /\ P_iP_t$. When the capture probability is relatively small, $U_{ms}\ /\ U_m$ is close to one, while it gradually reduces with $P_c\ /\ P_t$ increasing. When the relative time is allowed to increase beyond the upper limit given by Equation 23, as expected, $U_{ms}\ /\ U_m$ further decreases. On the

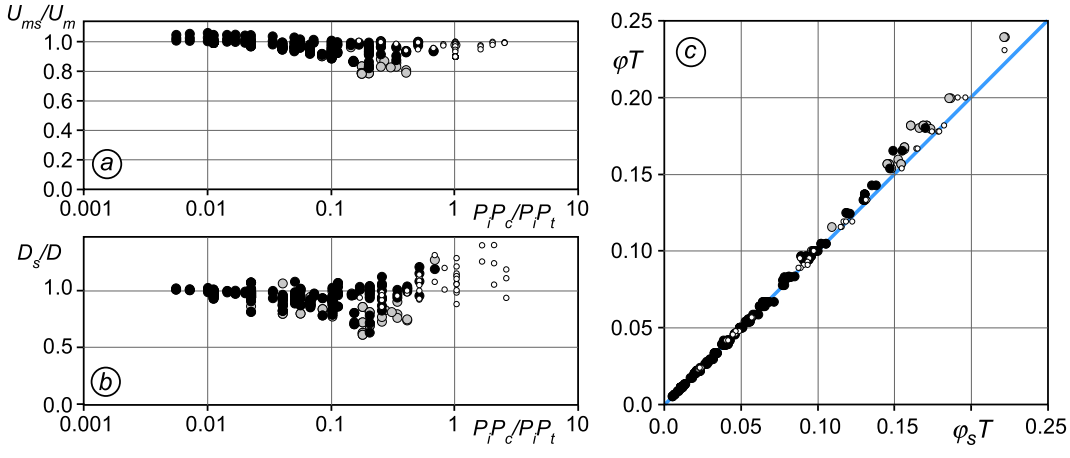

Figure 9. *a*) The ratio between the transport velocity computed with the stochastic model, U_{ms}, and the one given by Equation 5, as a funtion of $P_iP_c\ /\ P_iP_t$; *b*) the ratio between the diffusion coefficient computed with the stochastic model, D_s, and the one given by Equation 18, as a function of $P_iP_c\ /\ P_iP_t$; *c*) the non-dimensional capture rate coefficient given by Equation 19, φT, against the one computed with the stochastic model, $\varphi_s T$.

Table 1
Parameters of the Eulerian Model Estimated From the Experimental Results of Defina and Peruzzo (2012)

exp.	P_iP_c	P_iP_t	Δs (cm)	T (s)	U (cm/s)	U_m (cm/s)	D (cm^2/s)	D_t (cm^2/s)
*B*1	0.394	0.060	10.7	90	3.3	0.88	48.8	0.2
*B*2	0.287	0.065	10.7	88	5.0	1.06	74.1	0.3
*B*3	0.130	0.049	10.7	85	6.7	1.68	175.4	0.4
*B*6	0.047	0.032	10.7	80	13.3	3.06	568.2	0.8

Note. exp. denotes the same label of experiments as the One reported in Table 1 of Defina and Peruzzo (2012); U_m is the transport velocity computed with Equation 5, D is the diffusion coefficient computed with Equation 18, and D_t is the diffusion coefficient computed with the model proposed by Nepf (1999).

contrary, when the lower boundary for t / T given by Equation 21 is violated, the ratio U_{ms} / U_m remains close to one; the reason for this behavior is that the transport velocity is nearly equal to the velocity U when t / T is small because particles experienced only a small number of long time trapping events; therefore $U_{ms} \approx U_m \approx U$.

The same reasoning explains the behavior of the diffusion coefficient shown in Figure 9b when the lower limit for the relative time is satisfied. When constraint Equation 21 is violated, that is, when t / T is small, the diffusion coefficient computed using the results of the Lagrangian model is larger than that predicted by Equation 18, because the rates of temporarily retained and resumed particles are far from being in equilibrium and the spatial variance increases more than linearly with time.

The capture rate coefficient, φ, is weakly affected by the long time trapping events; Figure 9c confirms that Equation 19 predicts accurately the particle removal rate when $\varphi T < 0.1$; some inaccuracies can be observed only when $\varphi T > 0.15$; however, at this removal rate, the fraction of captured particles increases very quickly. For instance, with $\varphi T = 0.15$, Equation 22 predicts that more than 75% of the particles initially released is permanently captured at $t / T = 10$, and more then 99% is permanently captured at $t / T = 30$. Accordingly, the inaccuracy in estimating the rate of capture by Equation 22 is not significant.

On the whole, given the large uncertainties that typically affect the estimation of the transport velocity and diffusion coefficient when dealing with the flow through vegetated areas, we can conclude that Equation 19 can confidently be used to assess the parameters of a standard transport and diffusion model for particles propagating through emergent vegetation.

Comparison with available experimental results. As mentioned in Section 2, we use the experimental results of Defina and Peruzzo (2012) to show that, in flow regimes typically observed in natural wetlands, the transport velocity can be much smaller than the flow velocity and the diffusion coefficient can be much greater than that found for turbulent diffusion and mechanical dispersion. Defina and Peruzzo (2012) reported a series of experiments on the propagation of floating particles through emergent vegetation. The experiments were carried out in a 6 m long flume and the model plant canopy consisted of plastic plants, randomly arranged over a 3 m long test section; plant density was $n_p = 86.7$ m^{-2}, and hence $\Delta s = 0.107$ m, and bulk flow velocity was in the range $U = 3.3 - 13.3$ cm/s. Wooden particles were released just upstream of the canopy and their paths through the vegetation were recorded by a camera to estimate the probabilities P_i, P_c, P_t, and the duration, T, of temporary trapping events. The results of these experiments are summarized in Table 1.

Using Equations 5 and 18, we find a transport velocity, U_m, in the range from 0.88 to 3.06 cm/s and a diffusion coefficient, D, in the range from 50 to 570 cm^2/s, respectively. It is worth noting in Table 1, that the transport velocity, U_m, is up to five times smaller than the flow velocity, U.

We also estimate the diffusion coefficient due to turbulence and mechanical dispersion using the model proposed by Nepf (1999); for this purpose we recall that each plastic plant used in the experiments by Defina and Peruzzo (2012) was composed of approximately 120 leaves with a diameter $d \approx 2$ mm; accordingly, the

number of leaves per unit area is $n \approx 10400\ m^{-2}$. Using these data with Equation 8 of Nepf (1999) we find the diffusion coefficients D_t listed in Table 1 that turns out to be dramatically smaller than those produced by the temporary trapping mechanism. The temporary trapping is hence the main mechanism promoting the longitudinal dispersion of seeds. This is further confirmed by comparing the results of the experiments performed by Defina and Peruzzo (2012) with those performed by Liu et al. (2020), in the same hydrodynamic condition, and in which the longitudinal dispersion depends on the slow-down of particles colliding with the stems. Liu et al. (2020) estimated coefficients of dispersion ranging from 2 to 4 cm^2/s, that are much smaller than those induced by long-time temporary trapping (see Table 1).

Interestingly, the scheme here proposed is effective also when considering slow-down processes or, equivalently, short-time trapping mechanisms. Nepf, Mugnier, and Zavistoski (1997) measured the longitudinal dispersion coefficient by releasing a conservative solute through an array of cylinders. In these experiments the mean flow velocity was $U \approx 6$ cm/s and the cylinders, with a diameter $d = 6$ mm, were randomly distributed with density $n = 1530\ m^{-2}$. They also found a mean transport velocity $U_m \approx 5.5$ cm/s and a dispersion coefficient $D = 1.2 \pm 0.4\ cm^2/s$. The delay of the solute particles propagation was mainly related to their trapping in the wake behind each cylinder. Accordingly, the mean retention time is likely comparable to the mean period of vortex shedding; with a cylinder Reynolds number $Re_d \approx 360$, the Strouhal number is $St \approx 0.2$ and hence $T \approx d / USt = 0.5$ s. On assuming that the probability that the solute particles being trapped in the wake behind a cylinder, that is, the probability P_iP_t, is given by the fraction of volume occupied by the wakes, we have $P_iP_t \approx 0.06$. With these estimates, Equations 5 and 18 give $U_m = 5.6$ cm/s and $D = 1.0\ cm^2/s$, respectively. Both these values compare favorably with those found in the experiments.

4. Conclusions

This paper presents an Eulerian model for the advection, diffusion, and removal of buoyant particles within regions of emergent vegetation. The model parameters are estimated based on the parameters of the more detailed stochastic Lagrangian model proposed by Defina and Peruzzo (2010, 2012) and suitably designed for the same purpose.

The impact of the temporary trapping events on the advection and diffusion of the floating particles is very large. On one hand, the transport velocity dramatically reduces compared to the bulk flow velocity. On the other hand, the diffusion largely increases resulting in dispersion coefficients dramatically larger than those predicted by the classical mechanical dispersion theory (e.g., Nepf, Mugnier, and Zavistoski (1997)).

When the permanent capture by vegetation is inhibited, the proposed relationships between the parameters of the Lagrangian stochastic model and those of the Eulerian model are very accurate. On the contrary, in the contemporary presence of diffusion and permanent capture events,a standard advection-diffusion model could not be strictly used to describe the propagation of floating particles through emergent vegetation. In this condition, the parameters of the model become time-dependent, see, for example, the transport velocity, U_m, in Figure 8. Nevertheless, the impact of time dependency is relatively small and the solution given by the proposed relationships satisfactorily predicts the Lagrangian propagation of floating particles through emergent vegetation; in most of the investigated conditions the error is smaller than 15%.

The time dependence of the parameters of the Eulerian model in the presence of permanent capture events is an interesting and important issue. It deserves further investigation in order to model floating particle dispersion through vegetation more accurately.

Data Availability Statement

The data used in this study are available at http://researchdata.cab.unipd.it/id/eprint/427.

Acknowledgments
This work was supported by the China Scholarship Council (CSC) (grant No.201806040205). We also acknowledge Martina Raffagnato for her contribution to a large number of simulations performed with the stochastic model. Open access funding enabled and organized by Projekt DEAL.

References

Chambert, S., & James, C. (2009). Sorting of seeds by hydrochory. *River Research and Applications*, *25*(1), 48–61. https://doi.org/10.1002/rra.1093

Chang, E. R., Veeneklaas, R. M., Buitenwerf, R., Bakker, J. P., & Bouma, T. J. (2008). To move or not to move: Determinants of seed retention in a tidal marsh. *Functional Ecology*, *22*(4), 720–727. https://doi.org/10.1111/j.1365-2435.2008.01434.x

Cunnings, A., Johnson, E., & Martin, Y. (2016). Fluvial seed dispersal of riparian trees: Transport and depositional processes. *Earth Surface Processes and Landforms*, *41*(5), 615–625. https://doi.org/10.1002/esp.3850

Defina, A., & Peruzzo, P. (2010). Floating particle trapping and diffusion in vegetated open channel flow. *Water Resources Research*, *46*(11), W11525. https://doi.org/10.1029/2010wr009353

Defina, A., & Peruzzo, P. (2012). Diffusion of floating particles in flow through emergent vegetation: Further experimental investigation. *Water Resources Research*, *48*(3), W03501. https://doi.org/10.1029/2011wr011147

Espinosa-Gayosso, A., Ghisalberti, M., Ivey, G. N., & Jones, N. L. (2013). Particle capture by a circular cylinder in the vortex-shedding regime. *Journal of Fluid Mechanics*, *733*, 171–188. https://doi.org/10.1017/jfm.2013.407

Espinosa-Gayosso, A., Ghisalberti, M., Ivey, G. N., & Jones, N. L. (2015). Density-ratio effects on the capture of suspended particles in aquatic systems. *Journal of Fluid Mechanics*, *783*, 191–210. https://doi.org/10.1017/jfm.2015.557

Fischer, H., List, E., Koh, R., Imberger, J., & Brooks, N. (1979). *Mixing in inland and coastal waters* (pp. 229–278). academic press. https://doi.org/10.1016/b978-0-08-051177-1.50011-8

Liu, X., Zeng, Y., & Huai, W. (2018). Modeling of interactions between floating particles and emergent stems in slow open channel flow. *Water Resources Research*, *54*(9), 7061–7075. https://doi.org/10.1029/2018wr022617

Liu, X., Zeng, Y., Katul, G., Huai, W., & Bai, Y. (2020). Longitudinal dispersal properties of floating seeds within open-channel flows covered by emergent vegetation. *Advances in Water Resources*, *144*, 103705. https://doi.org/10.1016/j.advwatres.2020.103705

Merritt, D. M., & Wohl, E. E. (2002). Processes governing hydrochory along rivers: Hydraulics, hydrology, and dispersal phenology. *Ecological Applications*, *12*(4), 1071–1087. https://doi.org/10.1890/1051-0761(2002)012[1071:pgharh]2.0.co;2

Nathan, R., & Muller-Landau, H. C. (2000). Spatial patterns of seed dispersal, their determinants and consequences for recruitment. *Trends in Ecology & Evolution*, *15*(7), 278–285. https://doi.org/10.1016/s0169-5347(00)01874-7

Nepf, H. (1999). Drag, turbulence, and diffusion in flow through emergent vegetation. *Water Resources Research*, *35*(2), 479–489. https://doi.org/10.1029/1998wr900069

Nepf, H., Mugnier, C., & Zavistoski, R. (1997). The effects of vegetation on longitudinal dispersion. *Estuarine, Coastal and Shelf Science*, *44*(6), 675–684. https://doi.org/10.1006/ecss.1996.0169

Nepf, H., Sullivan, J., & Zavistoski, R. (1997). A model for diffusion within emergent vegetation. *Limnology & Oceanography*, *42*(8), 1735–1745. https://doi.org/10.4319/lo.1997.42.8.1735

Nilsson, C., Brown, R. L., Jansson, R., & Merritt, D. M. (2010). The role of hydrochory in structuring riparian and wetland vegetation. *Biological Reviews*, *85*(4), 837–858. https://doi.org/10.1111/j.1469-185x.2010.00129.x

Nitto, D. D., Erftemeijer, P., Van Beek, J., Dahdouh-Guebas, F., Higazi, L., Quisthoudt, K., et al. (2013). Modelling drivers of mangrove propagule dispersal and restoration of abandoned shrimp farms. *Biogeosciences*, *10*(7), 5095–5113. https://doi.org/10.5194/bg-10-5095-2013

Palmer, M. R., Nepf, H. M., Pettersson, T. J., & Ackerman, J. D. (2004). Observations of particle capture on a cylindrical collector: Implications for particle accumulation and removal in aquatic systems. *Limnology & Oceanography*, *49*(1), 76–85. https://doi.org/10.4319/lo.2004.49.1.0076

Peruzzo, P., Defina, A., & Nepf, H. (2012). Capillary trapping of buoyant particles within regions of emergent vegetation. *Water Resources Research*, *48*(7), W07512. https://doi.org/10.1029/2012wr011944

Peruzzo, P., Defina, A., Nepf, H. M., & Stocker, R. (2013). Capillary interception of floating particles by surface-piercing vegetation. *Physical Review Letters*, *111*(16), 164501. https://doi.org/10.1103/physrevlett.111.164501

Peruzzo, P., Viero, D. P., & Defina, A. (2016). A semi-empirical model to predict the probability of capture of buoyant particles by a cylindrical collector through capillarity. *Advances in Water Resources*, *97*, 168–174. https://doi.org/10.1016/j.advwatres.2016.09.006

Peterson, J. M., & Bell, S. S. (2012). Tidal events and salt-marsh structure influence black mangrove (avicennia germinans) recruitment across an ecotone. *Ecology*, *93*(7), 1648–1658. https://doi.org/10.1890/11-1430.1

Richards, S. A., Possingham, H. P., & Noye, B. (1995). Larval dispersion along a straight coast with tidal currents: Complex distribution patterns from a simple model. *Marine Ecology Progress Series*, *122*, 59–71. https://doi.org/10.3354/meps122059

Rubenstein, D. I., & Koehl, M. A. (1977). The mechanisms of filter feeding: Some theoretical considerations. *The American Naturalist*, *111*(981), 981–994. https://doi.org/10.1086/283227

Rutherford, J. C. (1994). *River mixing*. John Wiley & Son Limited.

Shi, W., Shao, D., Gualtieri, C., Purnama, A., & Cui, B. (2020). Modelling long-distance floating seed dispersal in salt marsh tidal channels. *Ecohydrology*, *13*(1), e2157. https://doi.org/10.1002/eco.2157

Shimeta, J., & Jumars, P. A. (1991). Physical mechanisms and rates of particle capture by suspension feeders. *Oceanography and Marine Biology an Annual Review*, *29*(19), l–257.

Vella, D., & Mahadevan, L. (2005). The "cheerios effect". *American Journal of Physics*, *73*(9), 817–825. https://doi.org/10.1119/1.1898523

White, B. L., & Nepf, H. M. (2003). Scalar transport in random cylinder arrays at moderate Reynolds number. *Journal of Fluid Mechanics*, *487*, 43–79. https://doi.org/10.1017/s0022112003004579